Published in final edited form as:
Neuroimage. 2011 July 1; 57(1): 214–224. doi:10.1016/j.neuroimage.2011.04.003.

Developmental Change in Regional Brain Structure over 7 Months in Early Adolescence: Comparison of Approaches for Longitudinal Atlas-based Parcellation

Edith V. Sullivan[1], **Adolf Pfefferbaum**[1,2], **Torsten Rohlfing**[2], **Fiona C. Baker**[3,4], **Mayra L. Padilla**[2,3], and **Ian M. Colrain**[3,5]

[1]Department of Psychiatry & Behavioral Sciences, Stanford University School of Medicine, Stanford, CA

[2]Neuroscience Program SRI International, Menlo Park, CA

[3]Human Sleep Laboratory, SRI International, Menlo Park, CA

[4]Brain Function Research Group, School of Physiology, University of the Witwatersrand, Johannesburg, South Africa

[5]Department of Psychological Sciences, University of Melbourne, Parkville, Australia

Abstract

Early adolescence is a time of rapid change in neuroanatomy and sexual development. Precision in tracking changes in brain morphology with structural MRI requires image segmentation with minimal error. Here, we compared two approaches to achieve segmentation by image registration with an atlas to quantify regional brain structural development over a 7-month interval in normal, early adolescent boys and girls. Adolescents were scanned twice (average interval=7.3 months), yielding adequate data for analysis in 16 boys (baseline age 10.9 to 13.9 years; Tanner Stage=1 to 4) and 12 girls (baseline age=11.2 to 13.7 years; Tanner Stage=3 to 4). Brain volumes were derived from T1-weighted (SPGR) images and dual-echo Fast Spin-Echo (FSE) images collected on a GE 3T scanner with an 8-channel phased-array head coil and analyzed by registration-based parcellation using the SRI24 atlas. The “independent” method required two inter-subject registrations: both baseline (MRI 1) to atlas and follow-up (MRI 2) to the atlas. The “sequential” method required one inter-subject registration, which was MRI 1 to the atlas, and one intra-subject registration, which was MRI 2 to MRI 1. Gray matter/white matter/CSF were segmented in both MRI-1 and MRI-2 using FSL FAST with tissue priors also based on the SRI24 atlas. Gray matter volumes were derived for 10 cortical regions, gray+white matter volumes for 5 subcortical structures, and CSF volumes for 4 ventricular regions and the cortical sulci. Across the 15 tissue regions, the coefficient of variation (CV) of change scores across individuals was significantly lower for the sequential method (CV=3.02), requiring only one inter-subject registration, than for the independent method (CV=9.43), requiring two inter-subject registrations. Volume change based on the sequential method revealed that total supratentorial and CSF volumes increased,

Correspondence Adolf Pfefferbaum, M.D. Director, Neuroscience Program SRI International 333 Ravenswood Avenue Menlo Park, CA 94025 dolf@synapse.sri.com.

Statement on conflict of interest Drs. Sullivan, Pfefferbaum, Rohlfing, Baker, Padilla, and Colrain have no conflicts of interest with this work, either financial or otherwise.

while cortical gray matter volumes declined significantly ($p<.01$) in anterior (lateral and medial frontal, anterior cingulate, precuneus, and parietal) but not posterior (occipital, calcarine) cortical regions. These volume changes occurred in all boys and girls who advanced a step in Tanner staging. Subcortical structures did not show consistent changes. Thus, longitudinal MRI assessment using robust registration methods is sufficiently sensitive to identify significant regional brain changes over a 7-month interval in boys and girls in early adolescence. Increasing the temporal resolution of the retest interval in longitudinal developmental studies could increase accuracy in timing of peak growth of regional brain tissue and refine our understanding of the neural mechanisms underlying the dynamic changes in brain structure throughout adolescence.

Keywords

adolescence; longitudinal; MRI; brain; development; atlas-based parcellation; image registration; puberty

Introduction

Adolescence is associated with continued growth of head size and substantial changes in regional brain structure. Over the last two decades, quantitative cross-sectional studies using structural magnetic resonance imaging (MRI) revealed a curvilinelar developmental trajectory of cortical gray matter with an increase from birth to about 10 years of age followed by a continuous decline through adulthood to old age (Bartzokis et al., 2001; Blanton et al., 2001; Blatter et al., 1995; Caviness et al., 1996; Courchesne et al., 2000; De Bellis et al., 2001; Giedd et al., 1996a; for reviews Giedd et al.; Giedd et al., 1996b; Gogtay et al., 2004; Jernigan et al., 2001; Jernigan and Tallal, 1990; Kennedy et al., 1998; Lange et al., 1997; Paus et al., 1999; Pfefferbaum et al., 1994; Raz, 2004; Raz and Rodrigue, 2006; Reiss et al., 1996; Sowell et al., 1999; Sowell et al., 2002; Stiles and Jernigan; Tisserand et al., 2002). A further theme of these studies was the presence of age-related differences in regional brain volumes, suggesting a posterior-to-anterior developmental order. Verification of these cross-sectional data and speculations required longitudinal study to calculate true developmental trajectories and individual differences by brain region and tissue type (Giedd et al., 1996a).

In general, prospective longitudinal studies (reviewed in Paus, 2010) have verified cross-sectional observations and have provided the essential data to model developmental trajectories of regional brain growth. In particular, developmental patterns derived from longitudinally-acquired T1-weighted MRI data indicate heterochronicity and trajectory differences by brain region and sex (Giedd et al., 1999; Lenroot et al., 2007; Sowell et al., 1999; Sowell et al., 2004b). The brain size of boys is typically upwards of 10% larger than that of girls (Dekaban and Sadowsky, 1978; Goldstein et al., 2001). Brain growth in girls starts and ends earlier than that in boys, peaking at 10.5 years in girls and 14.5 years in boys and declining thereafter (Lenroot et al., 2007). Regionally, the neocortex follows a curvilinear trajectory (Gogtay et al., 2004; Lenroot et al., 2007; Shaw et al., 2008), whereas allocortex and medial temporal structures follow a linear path (Gogtay et al., 2004). Growth in cortical regions is earlier for both sexes in posterior cortical than anterior regions, being about 7 to 10 years in occipital and parietal cortices and 10 to 13 years in frontal regions (Shaw et al., 2008).

While trajectories of growth curves provide a basis for estimating peaks in growth, the accuracy of the estimates is limited by temporal resolution of the measurements. The test-retest interval used in the large-scale longitudinal NIMH study of brain development, focused on ages 3.5 to 33 years old, is 2 years (Giedd et al., 1999; Giedd et al., 1996a). The

cohort of Sowell and colleagues (e.g., Sowell et al., 2004a; Sowell et al., 2002) was also scanned at 2-year intervals and focused on development of regional cortical thickness and presented novel findings on continued gray matter thinning of cortical language areas associated with vocabulary scores, an index of language development (Sowell et al., 2004a). Likewise, the NIH MRI study of normal brain development uses 2 year intervals for ages 7 days to 18.3 years old but introduced intervals as close as 3 months for children ages 7 days to 4.5 years to improve modeling of development during these years of rapid change (Evans, 2006).

These childhood-to-adolescent years also mark advancement through puberty and its plethora of sex-specific hormonal changes that influence physical growth and maturity not only in physiognomy but also in brain morphology. Despite the likely linking of pubertal and brain structural development, few MRI studies provide information about pubertal staging at times of study (cf., Blakemore et al.). Those that have used schedules of pubertal development, such as Tanner staging (Tanner, 1962), or direct measurement of sex hormones report mixed results, with some [MRI: (Neufang et al., 2009; Peper et al., 2009a)] but not others [sleep electrophysology: (Feinberg et al., 2006)] finding staging or hormonal levels to be predictive of changes in brain structure or presumed associated function. Whether brain structural changes are great enough for detection with conventional MRI over about half-year intervals in young adolescents has not been tested and therefore never linked to active pubertal advancement.

Accordingly, this study focused on change in regional brain volumes over an average of 7 months in adolescent boys and girls and identification of image quantification approaches that would be sensitive yet robust enough to detect changes reliably over this short interval. To calculate volume change using atlas-based image segmentation with the SRI24 atlas (Rohlfing et al., 2010), two principal image registration approaches were tested. The “independent” method required two inter-subject registrations to the atlas: both baseline (MRI 1) to the atlas and follow-up (MRI 2) to the atlas. The “sequential” method required one inter-subject registration, which was MRI 1 to the atlas, and one intra-subject registration, which was MRI 2 to MRI 1. We tested the hypothesis that the sequential approach for quantifying regional volume change would yield lower coefficients of variation (CV) of change scores across individuals than the independent method, rendering differences more reflective of true developmental effects rather than misregistration. Considering known growth patterns (Lenroot et al., 2007; Sowell et al., 2004a), we predicted that 1) cortical tissue volumes would decline, 2) ventricular and cortical sulcal volumes would expand, and 3) the sequential method of registration would detect these changes more readily than the independent method. As a test of convergent validity of the method, changes in regional brain volumes using each registration approach were correlated with changes observed in Tanner stages.

Methods

Subjects

Adolescents (11 to 14 years old) were recruited from the local community through flyers, word of mouth, and through advertisements placed in local school newsletters. Following school newsletters and with the approval of the administrations of each school, sleep laboratory staff gave a brief presentation to the adolescents during school time. The study was approved by the IRB at SRI International. Parents gave informed written approval for their children to participate and the children gave assent to participate in this longitudinal study. The procedures described next were conducted at the baseline visit and at follow-up, which occurred on average 7.3 months later (range=4 to 10.7 months).

At their initial and follow-up visits, parents and their children were interviewed by a laboratory research psychologist or other trained researcher using a structured interview (Kiddie Schedule for Affective Disorders, K-SADS) to assess current and lifetime history of psychiatric disorders (Kaufman et al., 1997). Using the probe questions of K-SADS-PL, the interviewer questioned each participant about age at first regular use of alcohol or drug and recency and frequency of use for each substance. No participant endorsed regular use of alcohol or any substance at baseline or follow-up. One parent of each child was also interviewed at each session and confirmed, without knowledge of the child's report, a negative history of regular alcohol and drug use. No further information on alcohol or drug misuse was obtained because there were no endorsements of gate (i.e., probe) questions. Other exclusionary criteria were history of loss of consciousness > 30 minutes or central nervous system diseases. Parents provided information to determine socioeconomic status (Hollingshead, 1975). Intelligence quotient (IQ) of each adolescent was measured with the Peabody Picture Vocabulary Test (Dunn and Dunn, 1997).

The adolescents were given the self-administered rating scale for pubertal development (Carskadon et al., 1993). Pubertal category scores for boys were based on body hair growth, voice change, and facial hair growth. Scores for girls were based on body hair growth, breast development, and menarche. Boys and girls were classified as pre-pubertal (Tanner 1), early pubertal (Tanner 2), mid-pubertal (Tanner 3), late pubertal (Tanner 4), or post-pubertal (Tanner 5) (Carskadon and Acebo, 1993), with stages in our sample ranging from 1 to 4. Demographic data appear in Table 1.

MRI acquisition

MR data were collected on a GE 3T Signa scanner with an 8-channel phased-array head coil. Brain volumes were derived from T1-weighted Inversion-Recovery Prepared SPoiled Gradient Recalled (SPGR) images (TR=7 ms, TE=2.2 ms, TI=300 ms, thick=1.25 mm, skip=0 mm, 124 slices, scan time=9:43 min) and dual-echo Fast Spin-Echo (FSE) images (TR=8583 ms, TE=13.5/108.3, thick= 2.5 mm, skip=0 mm, 62 slices).

Image preprocessing

All acquired structural images were first corrected for intensity bias by applying a second-order polynomial multiplicative bias field computed via entropy minimization (Likar et al., 2001). The late-echo FSE image was corrected using the bias field computed from the corresponding early-echo image to maintain the ratio of early- and late-echo values at each pixel, which keeps quantities derived from this ratio (e.g., T2) invariant. For each subject and each session, the bias-corrected early-echo FSE image was then registered to the bias-corrected SPGR image using intensity-based nonrigid image registration (Rohlfing and Maurer, 2003) (http://nitrc.org/projects/cmtk). The SPGR, early-echo FSE, and late-echo FSE images were each skull stripped using FSL's Brain Extraction Tool, BET (Smith, 2002). The early- and late-echo brain masks were reformatted into SPGR image space and combined with the SPGR-derived brain mask via label voting (Rohlfing and Maurer, 2005) to form the final SPGR brain mask.

Registration and atlas-based parcellation

For each subject, the skull-stripped baseline and follow-up SPGR images were each registered to the SPGR channel of the SRI24 atlas (Rohlfing et al., 2010) (http://nitrc.org/projects/sri24) via nonrigid image registration (Rohlfing and Maurer, 2003). We chose the SRI24 atlas over other available brain templates (e.g., MNI152) because of its ability to discern detailed anatomical structures, which can thus be unambiguously outlined directly in the atlas images without the need to access the images that were used to create the atlas itself. *Independent* cortical and subcortical parcellation maps for baseline and follow-

up images were obtained by reformatting labels maps defined in SRI24 directly into baseline and follow-up SPGR image spaces using the subject-to-atlas coordinate transformations.

The unstripped but bias-corrected follow-up SPGR image for each subject was then registered to the unstripped and bias-corrected baseline SPGR image. *Sequential* parcellation maps for the follow-up SPGR images were obtained by reformatting the SRI24 labels maps using the concatenation of follow-up-to-baseline and baseline-to-atlas transformations.

The rationale for using direct transformations to parcellate the baseline images, but concatenated transformations to obtain follow-up parcellation maps is the inevitable presence of registration errors. Because subject-to-atlas (i.e., inter-subject) registration is a relatively more difficult computational problem than within-subject longitudinal registration, we expected registration errors to be more severe in the former than the latter.

Thus, although the use of a concatenated transformation to parcellate the follow-up data does not eliminate subject-to-atlas registration errors, we ensure that the same errors apply to baseline and follow-up data consistently, which would not be the case if the follow-up data were registered to the atlas independently. Because we are primarily interested in measuring longitudinal effects, longitudinal consistency of registration errors should be beneficial. Finally, as a test of the robustness of the sequential approach we reversed the inter- and intra-subject chain and reformatted the SRI24 labels maps for the baseline images using the concatenation of baseline-to-followup and followup-to-atlas transformations.

Tissue segmentation

All bias-corrected and skull-stripped SPGR images were segmented into three tissue compartments (gray matter, white matter, CSF) using FSL's FAST tool (Zhang et al., 2001). As tissue priors to both initialize and guide the classification, we used the tissue probability maps provided with the SRI24 atlas, reformatted into subject SPGR space via the same transformations described above for the independent atlas-based parcellation.

Regions of interest (ROIs)

This analysis focused on major lobar tissue regions of the cortex, allocortex, and subcortical structures. Accordingly, the 116 ROIs available from the SRI24 atlas, derived from the Automated Anatomical Labelling (AAL) template (Tzourio-Mazoyer et al., 2002) were collapsed into 15 bilateral ROIs (Figure 2). The decision to collapse the 116 ROIs into 15 was motivated by considering the proportion of ROIs (N=15) to subjects (N=28) and confirmed by the use of these 15 ROIs in our studies of cerebrovascular perfusion (Pfefferbaum et al., 2011; Pfefferbaum et al., 2010). A further consideration was the desire to have anatomically-driven tissue subregions, and not simply gross lobar volumes, that were of similar size for statistical comparability. For each subject and time, gray matter volume was computed for each cortical region, and tissue volume for each subcortical region. Also measured were CSF-filled volumes of the lateral ventricles, third ventricle, temporal horns, cortical sulci, and sylvian fissures, based on ROIs drawn also on the SRI24 SPGR template (Figure 3) and reformatted into subject image space. The ventricles were identified by registration, and for the cortical sulci and sylvian fissure, the CSF segmentations from FAST were multiplied against the ROIs in Figure 3.

ROI to estimate signal-to-noise ratio (SNR)

We estimated SNR, which could be diminished by subject movement, in a sample of highly coherent white matter in the centrum semiovale of the inner 55% of the supratentorium masked on the SRI24 atlas and applied to each individual's MRI at each session. This white matter region, which was approximately 110 cc volume across subjects, began inferiorly at

midpons, extended superiorly to the superior reaches of the centrum semiovale, just inferior to the cortical gyri and sulci, and medially to the sylvian fissures and excluded the corpus callosum. To further ensure homogeneity of tissue, the region was also masked by each individual scan's white matter segmentation. SNR was calculated as the mean divided by the standard deviation of the signal intensity of all voxels in this white matter sample.

Statistical analysis for MRI data

Comparison of the two registration methods was based on differences between volumes at MRI 1 (baseline) and MRI 2 (followup) derived from each method. Because tissue volumes were predicted to decline and CSF volumes were predicted to increase, differences were tested with one-tailed paired t-tests and with family-wise Bonferroni correction; thus for 15 tissue ROIs, the critical p-value = .007, and for the 5 CSF volume ROIs, the critical p-value = .02.

Coefficients of variation (CV) of change scores across individuals were calculated for each ROI determined from each method, where the CV=SD/mean of the 15 tissue ROIs. CVs provide a measure of the dispersion of the values with respect to the mean expressed as a percentage and serve as an index of measurement precision. As such, the CV is an error estimate, which can reflect parcellation, registration, movement, and other sources of error. Mean CVs across the 15 tissue ROIs were derived for each registration method and compared with Wilcoxon tests. The same analysis procedure was conducted for CSF volumes of the ventricles and cortical sulci. The method with the lower CVs was then chosen to describe regional brain changes with development using paired t-tests or Mann-Whitney U-tests and Pearson correlations or Spearman rank order tests between change in regional brain volumes and change in Tanner stage.

Results

Comparison of the sequential and independent registration methods

Tissue ROIs—Change measured in the 15 tissue ROIs revealed similar patterns regardless of registration method (Figure 4). For the sequential method, significant declines in volumes were present in five regions: lateral frontal (p=.0001), medial frontal (p=.0002), anterior cingulate (p=.01), precuneus (p=.0006), and parietal (p=.0001) cortices; the temporal cortex showed a trend (p=.02). For the independent method, significant declines in volumes were present in four regions: lateral frontal (p=.0005), medial frontal (p=.0063), precuneus (p=.0014), and parietal cortices (p=.0011).

Across the 15 tissue ROIs, the CV for the sequential method was 3.0% and for the independent method was 9.4%. This difference was significant with the Wilcoxon test (Z=2.953, p=.0031), favoring the sequential method. As a further test of the robustness of the sequential method, we reversed the temporal order of the intra-subject registration with the SRI24 atlas, so that the reformatting sequence was SRI24 - MRI 2 - MRI 1. The average CVs for this reversed sequence was 4.2% and also was significantly lower than that of the direct method (Z=2.272, p=.0231) but not significantly different from that of the forward sequential method (Z=0.568, p=.5701). The CVs for the ICV was 9.7% for both the direct and sequential methods.

CSF-filled ROIs—For the sequential method in the forward direction, increases in the CSF-filled volumes were significant in four of the five ROIs: lateral ventricles (p=.0017), temporal horn (p=.0006), cortical sulci (p=.0001), and sylvian fissures (p=.0038); the enlargement of the third ventricle was not significant (p=.1300). For the independent method, although all CSF ROIs increased over time, three did so significantly: lateral

ventricles (p=.0014), cortical sulci (p=.0030), and sylvian fissures (p=.0038); the enlargement of neither the third ventricle (p=.0420) nor temporal horns (p=.1971) was significant.

Although the mean CVs across the five CSF ROIs was lower with the sequential (2.1%) than independent (2.9%) method, this difference was not significant (Z=.405, p=.6858). Supratentorial volume showed a greater increase with the sequential method (mean ±SD=12.23±13.11 cc, p=.0001) and lower CV (10.7%) than with the independent method (6.36±12.06 cc, p=.0095; CV=18.9%).

SNR by registration method—The SNR for each registration method at each MRI was about the same: MRI 1=10.58 and MRI 2=10.55 for the independent method; MRI 1=10.58 and MRI 2 =10.57 for the forward sequential method; and MRI 1=10.49 and MRI 2=10.55 for the backward sequential method. None differed significantly between scans within a method. Further, none of the SNR estimates correlated significantly with age, and none differed by sex.

ROI volume change based on sequential registration

Assuming that the CVs reflect measurement error, the results indicated that the sequential method (temporally forward) yielded lower error than the independent method in longitudinal data analysis and thus was used in the remaining analyses to characterize developmental change in regional brain volume over the rescan interval. ROIs exhibiting significant volume changes from MRI 1 to MRI 2 are presented as “spaghetti” plots (Figures 5–7 and Table 2).

The supratentorial volume increased about 1.0% (p<.0001). The average supratentorial volume of the boys was larger than that of the girls at both MRIs (p=.0001), but percentage volume change (boys=1.0% vs. girls=0.8%) was not related to sex (t(26)=6.97, p=.49) or BMI (r=−.22, p=.25). Similarly for the tissue and CSF ROIs, the boys generally had larger volumes than the girls, but there were no significant differences between boys and girls in percentage change for any of the 21 ROIs (the largest t-value=1.375, p=.1809).

Longer time between MRIs correlated with greater volume declines in several cortical gray matter ROIs: lateral frontal (r=−.44, p=.0202), precuneus (r=−.62, p=.0004), and parietal (r=−.43, p=.0239) volumes. Using multiple regression, we attempted to discern whether these relations were attributable to length of interval or to age at MRI 1 and found that interval length made an independent contribution to the volume changes (p=.0235 for lateral frontal, p=.0004 for precuneus, and p=.0264 for parietal volumes) over and above the contribution from age.

Longer intervals between MRI sessions could herald advance in Tanner stage. Of the 28 adolescents, 5 advanced by one step: 3 girls changed from 3 to 4, and 2 boys changed from 2 to 3. Consistent with the known developmental pattern, all 5 adolescents who advanced by Tanner stage showed volume loss in lateral frontal, anterior cingulate, precuneus, and parietal gray matter and expansion of the lateral ventricles and cortical sulci (Figure 8). Of these 6 regions, Mann-Whitney tests indicated a decline (one-tailed) in anterior cingulate (p=.0223) and precuneus (p=.0256) gray matter volume and an increase in cortical sulcal volume (p=.0223) in the 5 who changed compared with those who did not.

Discussion

The results of this study provide evidence that longitudinal MRI assessment using robust registration is sufficiently sensitive to identify significant regional brain changes over about

a half-year in boys and girls in early adolescence. The independent registration method used two inter-subject registration steps, whereas the sequential registration method relied on one inter-subject and one intra-subject registration. Reducing the number of inter-subject registrations minimized measurement error, as revealed by the lower CV for the sequential than independent methods, and likely enhanced detection of small volume changes occurring over short intervals. Consistent with current longitudinal studies based on longer follow-up intervals, the patterns of change differed by brain region. Specifically, developmental changes were greater in anterior than posterior cortex, suggesting remodeling of brain structure towards maturity (Gogtay et al., 2004; Sowell et al., 2004a). As with all in vivo imaging protocols, precision and registration are limited by the spatial resolution of acquired images, which in our case was about 1 mm^3.

Adolescent neurodevelopmental trajectories show a dynamic, complex, and predictable change, with regionally different rises and falls in volume or cortical thickness notable in the age range between 7 and 18 years but with most changes occurring between 9 and 13 years. These neurodevelopmental trajectories were established from data typically collected at 2-year intervals (Lenroot and Giedd, 2010; Shaw et al., 2008), although the NIH-PD study adjusts its interval by age, where infants and children age 7 days to 4 years are scanned up to 5 times at 3 or more month intervals, whereas children to adolescents age 5–18 years are scanned 3 times in 2-year intervals (Evans, 2006). In the NIH-CHPB longitudinal study, Lenroot et al. (Lenroot et al., 2007) reported on 387 boys and girls and men and women, age 3 to 27 years, and showed that total cortical gray matter volume peaked at 10.5 years in girls and 14.5 years in boys. Cortical frontal gray matter volume of girls peaks about a year before that of boys (10.5 compared with 11.5 years of age). This sex-related difference in volume peak was slightly earlier than those reported in an earlier study from the same research group based on fewer adolescents for whom the peaks were at 11 years of age for girls and 12.1 years for boys (Giedd et al., 1999). Shaw et al. (Shaw et al., 2008) reported on 375 youth and adults of the NIH-CHPB cohort, age 3.5 to 33 years, and a total of 764 MRIs collected longitudinally at 2-year intervals. Age of peak cortical thickness of different frontal regions ranged between 9.6 years for precentral cortex to 13.8 years for the cingulate cortex. Cortical brain regions have characteristically different cell types and structures and followed different growth trajectories, for example, cubic for neo (iso) cortex and linear for allocortex. Our increased “temporal” resolution of image acquisition was sensitive enough to detect a 2% decline in anterior cortical volume. The implication of this ability suggests that narrowing the retest interval should increase accuracy in timing of peak growth of regional brain tissue and refine modeling of individual variability in the time and slope of regional neurodevelopmental trajectories notable in the “spaghetti” plots.

A robust factor in regional brain structural change in the present study was pubertal advancement as measured by self-reported Tanner staging. Advancing a step in Tanner stage heralded declines in lateral frontal, anterior cingulate, precuneus, and parietal gray matter volumes and expansion of the lateral ventricles and cortical sulci. Volume changes were uniquely related to scan interval rather than to age. Despite limitations of self-reported Tanner stage determination, this method is still considered valid (Duke et al., 1980) and a“gold standard” (Dorn et al., 2006). Although as noted by Luna et al. (Luna et al., 2010) the validity of self-reported Tanner staging can be affected by age, sex, ethnicity, race, and weight status (Bonat et al., 2002; Neinstein, 1982; Raman et al., 2009; Schlossberger et al., 1992), the young adolescents in the current study were of relatively high socioeconomic status, mostly Caucasian, and with normal BMI, factors that are associated with valid self-staging.

Other MRI studies accounting for pubertal development were cross-sectional. A VBM analysis of MRI data in 37 boys and 41 girls, age 10 to 15 years old, showed that smaller

total gray matter volumes correlated with higher estradiol levels in girls, notably in prefrontal, parietal, and middle temporal cortices; sex hormone-MRI volume correlations were not forthcoming in the boys, likely because they were, on average, about a year younger than the girls (Peper et al., 2009a). A twin study of 210, 9-year old boys and girls (Peper et al., 2009b) provided strong cross-sectional evidence, based on VBM analysis, for an association between pubertal development in children with secondary sexual characteristic and those without them and the onset of decreasing gray matter in prefrontal and parietal cortical density. Another cross-sectional MRI study in 15 boys and 15 girls with Tanner stage information and circulating hormone levels revealed a complex set of relations involving medial temporal and diencephalic brain structures that suggested a role for sex hormones in influencing the organization of brain development (Neufang et al., 2009).

A number of factors can affect image quality and registration accuracy and ultimately increase measurement error. Church et al. (Church et al., 2010) reviewed problems of head size differences and movement in the scanner as common problems to overcome in acquisition and analysis. They note, for example, that although children have smaller heads and tend to move more in the scanner than adults, these problems can be minimized by registering brains of all ages (especially those at least 7 years old) to a common atlas. This approach also enables direct comparison of children and adults, at least within the older child/young adolescent to adult age range (Burgund et al., 2002). In the current study, we used the SRI24 atlas (Rohlfing et al., 2010) constructed from adult MRI data to register the adolescent MRI data, collected in 10 to 13 year olds, into common space, thus abiding one of the recommendations to minimize error from subject movement. In addition, we calculated SNR in the MRIs for each registration approach and found adequate SNR for each method that was not related to age or sex. The sequential registration approach could also apply to functional studies, which require registration across image modalities within subjects and to standard spatial coordinate systems (i.e., atlases) as well as accounting for developmental changes in structure (cf., Poldrack, 2010).

The repeated observation of the ontogenetic progression of posterior to anterior brain development has engendered the interpretation that frontal regions exhibit more active synaptic pruning than posterior regions during early adolescence (Feinberg, 1983; Huttenlocher, 1979, 1990). The active changes in anterior neocortex and allocortex may well parallel known developmental changes that occur in executive functions, including attention, behavioral regulation, judgment, and problem solving as adolescents progress towards adulthood (for review, Stiles and Jernigan, 2010). It is tempting to speculate that narrowing the retest interval would increase accuracy in timing of peak growth of regional brain tissue and refine our understanding of the neural mechanisms underlying the dynamic changes in brain structure throughout adolescence.

Acknowledgments

This work was supported by NIH grants AA016273, AA005965, AA017168, AG017919, EB008381.

References

Bartzokis G, Beckson M, Lu PH, Nuechterlein KH, Edwards N, Mintz J. Age-related changes in frontal and temporal lobe volumes in men: a magnetic resonance imaging study. Archives of General Psychiatry. 2001; 58:461–465. [PubMed: 11343525]

Blakemore SJ, Burnett S, Dahl RE. The role of puberty in the developing adolescent brain. Hum Brain Mapp. 2010; 31:926–933. [PubMed: 20496383]

Blanton RE, Levitt JG, Thompson PM, Narr KL, Capetillo-Cunliffe L, Nobel A, Singerman JD, McCracken JT, Toga AW. Mapping cortical asymmetry and complexity patterns in normal children. Psychiatry Res. 2001; 107:29–43. [PubMed: 11472862]

Blatter DD, Bigler ED, Gale SD, Johnson SC, Anderson C, Burnett BM, Parker N, Kurth S, Horn S. Quantitative volumetric analysis of brain MRI: Normative database spanning five decades of life. American Journal of Neuroradiology. 1995; 16:241–245. [PubMed: 7726068]

Bonat S, Pathomvanich A, Keil MF, Field AE, Yanovski JA. Self-assessment of pubertal stage in overweight children. Pediatrics. 2002; 110:743–747. [PubMed: 12359788]

Burgund ED, Kang HC, Kelly JE, Buckner RL, Snyder AZ, Petersen SE, Schlaggar BL. The feasibility of a common stereotactic space for children and adults in fMRI studies of development. Neuroimage. 2002; 17:184–200. [PubMed: 12482076]

Carskadon MA, Acebo C. A self-administered rating scale for pubertal development. J Adolesc Health. 1993; 14:190–195. [PubMed: 8323929]

Carskadon MA, Vieira C, Acebo C. Association between puberty and delayed phase preference. Sleep. 1993; 16:258–262. [PubMed: 8506460]

Caviness VS, Kennedy DN, Richelme C, Rademacher J, Filipek PA. The human brain age 7–11 years: a volumetric analysis based on magnetic resonance images. Cerebral Cortex. 1996; 6:726–736. [PubMed: 8921207]

Church JA, Petersen SE, Schlaggar BL. The “Task B problem” and other considerations in developmental functional neuroimaging. Hum Brain Mapp. 2010; 31:852–862. [PubMed: 20496376]

Courchesne E, Chisum HJ, Townsend J, Cowles A, Covington J, Egaas B, Harwood M, Hinds S, Press GA. Normal brain development and aging: quantitative analysis at in vivo MR imaging in healthy volunteers. Radiology. 2000; 216:672–682. [PubMed: 10966694]

De Bellis MD, Keshavan MS, Beers SR, Hall J, Frustaci K, Masalehdan A, Noll J, Boring AM. Sex differences in brain maturation during childhood and adolescence. Cereb Cortex. 2001; 11:552–557. [PubMed: 11375916]

Dekaban A, Sadowsky D. Changes in brain weights during the span of human life: Relation of brain weights to body heights and body weights. Annals of Neurology. 1978; 4:345–356. [PubMed: 727739]

Dorn LD, Dahl RE, Woodward HR, Biro F. Defining the boundaries of early adolescence: A user's guide to assessing pubertal status and pubertal timing in research with adolescents. Applied Developmental Science. 2006; 10:30–56.

Duke PM, Litt IF, Gross RT. Adolescents' self-assessment of sexual maturation. Pediatrics. 1980; 66:918–920. [PubMed: 7454482]

Dunn, LM.; Dunn, ES. Peabody Picture Vocabulary Test - Third Edition. American Guidance Service; Circle Pines, MN: 1997.

Evans AC. The NIH MRI study of normal brain development. Neuroimage. 2006; 30:184–202. [PubMed: 16376577]

Feinberg I. Schizophrenia caused by a fault in programmed synaptic elimination during adolescence? Journal of Psychiatric Research. 1983; 17:319–334. [PubMed: 7187776]

Feinberg I, Higgins LM, Khaw WY, Campbell IG. The adolescent decline of NREM delta, an indicator of brain maturation, is linked to age and sex but not to pubertal stage. Am J Physiol Regul Integr Comp Physiol. 2006; 291:R1724–1729. [PubMed: 16857890]

Giedd JN, Blumenthal J, Jeffries NO, Castellanos FX, Liu H, Zijdenbos A, Paus T, Evans AC, Rapoport JL. Brain development during childhood and adolescence: a longitudinal MRI study [letter]. Nature Neuroscience. 1999; 2:861–863.

Giedd JN, Snell JW, Lange N, Rajapakse JC, Casey BJ, Kozuch PL, Vaituzis AC, Vauss YC, Hamburger SD, Kaysen D, Rapoport JL. Quantitative magnetic resonance imaging of human brain development: ages 4–18. Cerebral Cortex. 1996a; 6:551–560. [PubMed: 8670681]

Giedd JN, Stockman M, Weddle C, Liverpool M, Alexander-Bloch A, Wallace GL, Lee NR, Lalonde F, Lenroot RK. Anatomic magnetic resonance imaging of the developing child and adolescent brain and effects of genetic variation. Neuropsychol Rev. 2010; 20:349–361. [PubMed: 21069466]

Giedd JN, Vaituzis AC, Hamburger SD, Lange N, Rajapakse JC, Kaysen D, Vauss YC, Rapoport JL. Quantitative MRI of the temporal lobe, amygdala, and hippocampus in normal human development: ages 4–18 years. Journal of Comparative Neurology. 1996b; 366:223–230. [PubMed: 8698883]

Gogtay N, Giedd JN, Lusk L, Hayashi KM, Greenstein D, Vaituzis AC, Nugent TF 3rd, Herman DH, Clasen LS, Toga AW, Rapoport JL, Thompson PM. Dynamic mapping of human cortical development during childhood through early adulthood. Proc Natl Acad Sci U S A. 2004; 101:8174–8179. [PubMed: 15148381]

Goldstein JM, Seidman LJ, Horton NJ, Makris N, Kennedy DN, Caviness VS Jr. Faraone SV, Tsuang MT. Normal sexual dimorphism of the adult human brain assessed by in vivo magnetic resonance imaging. Cereb Cortex. 2001; 11:490–497. [PubMed: 11375910]

Hollingshead, A. Four-Factor Index of Social Status. Yale University, Department of Sociology; New Haven, CT: 1975.

Huttenlocher PR. Synaptic density in human frontal cortex: Developmental changes and effects of aging. Brain Research. 1979; 163:195–205. [PubMed: 427544]

Huttenlocher PR. Morphometric study of human cerebral cortex development. Neuropsychologia. 1990; 28:517–527. [PubMed: 2203993]

Jernigan TL, Archibald SL, Fennema-Notestine C, Gamst AC, Stout JC, Bonner J, Hesselink JR. Effects of age on tissues and regions of the cerebrum and cerebellum. Neurobiology of Aging. 2001; 22:581–594. [PubMed: 11445259]

Jernigan TL, Tallal P. Late childhood changes in brain morphology observable with MRI. Developmental Medicine and Child Neurology. 1990; 32:379–385. [PubMed: 2354751]

Kaufman J, Birmaher B, Brent D, Rao U, Flynn C, Moreci P, Williamson D, Ryan N. Schedule for Affective Disorders and Schizophrenia for School-Age Children-Present and Lifetime Version (K-SADS-PL): initial reliability and validity data. J Am Acad Child Adolesc Psychiatry. 1997; 36:980–988. [PubMed: 9204677]

Kennedy DN, Lange N, Makris N, Bates J, Meyer J, Caviness VS Jr. Gyri of the human neocortex: an MRI-based analysis of volume and variance. Cerebral Cortex. 1998; 8:372–384. [PubMed: 9651132]

Lange N, Giedd JN, Castellanos FX, Vaituzis AC, Rapoport JL. Variability of human brain structure size: Ages 4–20 years. Psychiatry Research Neuroimaging. 1997; 74:1–12.

Lenroot RK, Giedd JN. Sex differences in the adolescent brain. Brain Cogn. 2010; 72:46–55. [PubMed: 19913969]

Lenroot RK, Gogtay N, Greenstein DK, Wells EM, Wallace GL, Clasen LS, Blumenthal JD, Lerch J, Zijdenbos AP, Evans AC, Thompson PM, Giedd JN. Sexual dimorphism of brain developmental trajectories during childhood and adolescence. Neuroimage. 2007; 36:1065–1073. [PubMed: 17513132]

Likar B, Viergever MA, Pernus F. Retrospective correction of MR intensity inhomogeneity by information minimization. EEE Transactions on Medical Imaging. 2001; 20:1398–1410.

Luna B, Velanova K, Geier CF. Methodological approaches in developmental neuroimaging studies. Hum Brain Mapp. 2010; 31:863–871. [PubMed: 20496377]

Neinstein LS. Adolescent self-assessment of sexual maturation: reassessment and evaluation in a mixed ethnic urban population. Clin Pediatr (Phila). 1982; 21:482–484. [PubMed: 7083719]

Neufang S, Specht K, Hausmann M, Gunturkun O, Herpertz-Dahlmann B, Fink GR, Konrad K. Sex differences and the impact of steroid hormones on the developing human brain. Cereb Cortex. 2009; 19:464–473. [PubMed: 18550597]

Paus T. Population neuroscience: why and how. Hum Brain Mapp. 2010; 31:891–903. [PubMed: 20496380]

Paus T, Zijdenbos A, Worsley K, Collins DL, Blumenthal J, Giedd JN, Rapoport JL, Evans AC. Structural maturation of neural pathways in children and adolescents: In vivo study. Science. 1999; 283:1908–1911. [PubMed: 10082463]

Peper JS, Brouwer RM, Schnack HG, van Baal GC, van Leeuwen M, van den Berg SM, Delemarre-Van de Waal HA, Boomsma DI, Kahn RS, Hulshoff Pol HE. Sex steroids and brain structure in pubertal boys and girls. Psychoneuroendocrinology. 2009a; 34:332–342. [PubMed: 18980810]

Peper JS, Schnack HG, Brouwer RM, Van Baal GC, Pjetri E, Szekely E, van Leeuwen M, van den Berg SM, Collins DL, Evans AC, Boomsma DI, Kahn RS, Hulshoff Pol HE. Heritability of regional and global brain structure at the onset of puberty: a magnetic resonance imaging study in 9-year-old twin pairs. Hum Brain Mapp. 2009b; 30:2184–2196. [PubMed: 19294640]

Pfefferbaum A, Chanraud S, Pitel A-L, Müller-Oehring EM, Shankaranarayanan A, Alsop D, Rohlfing T, Sullivan EV. Cerebral blood flow in posterior cortical nodes of the default mode network decreases with task engagement but remains higher than in most brain regions. Cerebral Cortex. 2011; 21:233–244. [PubMed: 20484322]

Pfefferbaum A, Chanraud S, Pitel A-L, Shankaranarayanan A, Alsop DC, Rohlfing T, Sullivan EV. Volumetric cerebral perfusion imaging in healthy adults: Regional distribution, laterality, and repeatability of pulsed continuous arterial spin labeling (PCASL). Psychiatry Research: Neuroimaging. 2010; 182:266–273.

Pfefferbaum A, Mathalon DH, Sullivan EV, Rawles JM, Zipursky RB, Lim KO. A quantitative magnetic resonance imaging study of changes in brain morphology from infancy to late adulthood. Archives of Neurology. 1994; 51:874–887. [PubMed: 8080387]

Poldrack RA. Interpreting developmental changes in neuroimaging signals. Hum Brain Mapp. 2010; 31:872–878. [PubMed: 20496378]

Raman A, Lustig RH, Fitch M, Fleming SE. Accuracy of self-assessed Tanner staging against hormonal assessment of sexual maturation in overweight African-American children. J Pediatr Endocrinol Metab. 2009; 22:609–622. [PubMed: 19774842]

Raz, N. The aging brain observed in vivo: differential changes and their modifiers. In: Cabeza, R.; Nyberg, L.; Park, DC., editors. Cognitive Neuroscience of Aging:Linking Cogniitve and Cerebral Aging. Oxford University Press; New York: 2004. p. 17-55.

Raz N, Rodrigue KM. Differential aging of the brain: Patterns, cognitive correlates and modifiers. Neuroscience and Biobehavioral Reviews. 2006; 30:730–748. [PubMed: 16919333]

Reiss AL, Abrams MT, Singer HS, Ross JL, Denckla MB. Brain development, gender and IQ in children. A volumetric imaging study. Brain. 1996; 119:1763–1774. [PubMed: 8931596]

Rohlfing T, Maurer CR. Nonrigid image registration in shared-memory multiprocessor environments with application to brains, breasts, and bees. IEEE Transactions on Information Technology in Biomedicine. 2003; 7:16–25. [PubMed: 12670015]

Rohlfing T, Maurer CR. Multi-classifier framework for atlas-based image segmentation. Pattern Recognition Letters. 2005; 26:2070–2079.

Rohlfing T, Zahr NM, Sullivan EV, Pfefferbaum A. The SRI24 multi-channel atlas of normal adult human brain structure. Human Brain Mapping. 2010; 31:798–819. [PubMed: 20017133]

Schlossberger NM, Turner RA, Irwin CE Jr. Validity of self-report of pubertal maturation in early adolescents. J Adolesc Health. 1992; 13:109–113. [PubMed: 1627576]

Shaw P, Kabani NJ, Lerch JP, Eckstrand K, Lenroot R, Gogtay N, Greenstein D, Clasen L, Evans A, Rapoport JL, Giedd JN, Wise SP. Neurodevelopmental trajectories of the human cerebral cortex. J Neurosci. 2008; 28:3586–3594. [PubMed: 18385317]

Smith S. Fast robust automated brain extraction. Human Brain Mapping. 2002; 17:143–155. [PubMed: 12391568]

Sowell ER, Thompson PM, Holmes CJ, Jernigan TL, Toga AW. In vivo evidence for post-adolescent brain maturation in frontal and striatal regions [letter]. Nature & Neuroscience. 1999; 2:859–861.

Sowell ER, Thompson PM, Leonard CM, Welcome SE, Kan E, Toga AW. Longitudinal mapping of cortical thickness and brain growth in normal children. J Neurosci. 2004a; 24:8223–8231. [PubMed: 15385605]

Sowell ER, Thompson PM, Rex D, Kornsand D, Tessner KD, Jernigan TL, Toga AW. Mapping sulcal pattern asymmetry and local cortical surface gray matter distribution in vivo: maturation in perisylvian cortices. Cerebral Cortex. 2002; 12:17–26. [PubMed: 11734529]

Sowell ER, Thompson PM, Toga AW. Mapping changes in the human cortex throughout the span of life. Neuroscientist. 2004b; 10:372–392. [PubMed: 15271264]

Stiles J, Jernigan TL. The basics of brain development. Neuropsychol Rev. 2010; 20:327–348. [PubMed: 21042938]

Tanner, JM. Growth at Adolescence. Springfield, IL: 1962.

Tisserand DJ, Pruessner JC, Sanz Arigita EJ, van Boxtel MP, Evans AC, Jolles J, Uylings HB. Regional frontal cortical volumes decrease differentially in aging: an MRI study to compare volumetric approaches and voxel-based morphometry. NeuroImage. 2002; 17:657–669. [PubMed: 12377141]

Tzourio-Mazoyer N, Landeau B, Papathanassiou D, Crivello F, Etard O, Delcroix N, Mazoyer B, Joliot M. Automated anatomical labeling of activations in SPM using a macroscopic anatomical parcellation of the MNI MRI single-subject brain. NeuroImage. 2002; 15:273–289. [PubMed: 11771995]

Zhang Y, Brady M, Smith S. Segmentation of brain MR images through a hidden Markov random field model and the expectation maximization algorithm. IEEE Transactions Medical Imaging. 2001; 20:45–57.

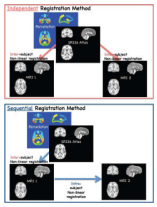

Figure 1.
Work flow of the independent (top) and sequential (bottom) registration method.

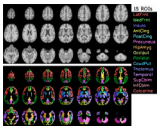

Figure 2.
Top panel in gray scale: Axial slices from the SRI24 atlas of the superior (top left) to inferior (bottom right) reaches of the brain. Bottom panel in color: 15 cortical and subcortical regions of interest (ROIs) overlaid on the SRI24 atlas and color-coded by structure name. LatFrnt=lateral frontal cortex; MedFrnt=medial frontal cortex; Insula; AntCing=anterior cingulate cortex; PostCing=posterior cingulate cortex; Precuneus; HipAmyg=hippocampus and amygdala; Occiput=occipital cortex; Parietal=parietal cortex; CaudPut=caudate and putamen; Thalamus; Temporal=temporal cortex; SupCblm=superior cerebellum; InfCblm=inferior cerebellum; Calcarine=calcarine cortex.

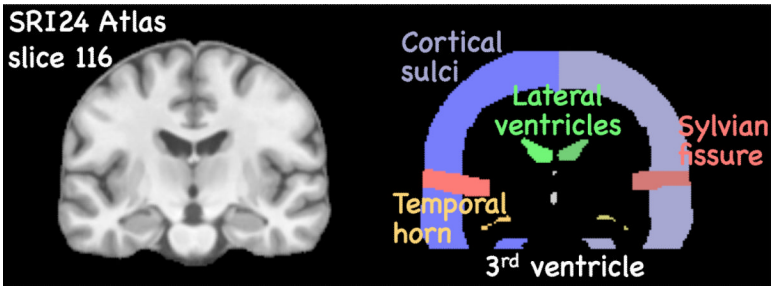

Figure 3.
Left panel in gray scale: Coronal slices from the SRI24 atlas at the level of the parcellated example. Right panel: 5 color-coded CSF-filled ROIs. Note that cortical sulcal volume was derived from the CSF volume in the outer 45% rim of the brain.

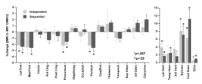

Figure 4.
Mean±SEM % regional volume change (%=(MRI 2 - MRI 1)/MRI 1) for tissue ROIs (top panel) and CSF-filled ROIs and supratentorial volume (SCV) (bottom panel) for the independent and sequential registration methods. Lat Frnt=lateral frontal cortex; Med Frnt=medial frontal cortex; Insula; Ant Cing=anterior cingulate cortex; Post Cing=posterior cingulate cortex; Precuneus; HippAmyg=hippocampus and amygdala; Occipital=occipital cortex; Parietal=parietal cortex; CaudPut=caudate and putamen; Thalamus; Temporal=temporal cortex; Sup Cblm=superior cerebellum; Inf Cblm=inferior cerebellum; Calcarine=calcarine cortex; Lat Vent=lateral ventricles; Temp Horn=temporal horn; 3rd Vent=third ventricle; Sylvian=sylvian fissures; Cort Sulci=cortical sulci; SVol=Supratentorial volume. * and † indicate ROIs showing significant differences of the percentage volume change from 0.

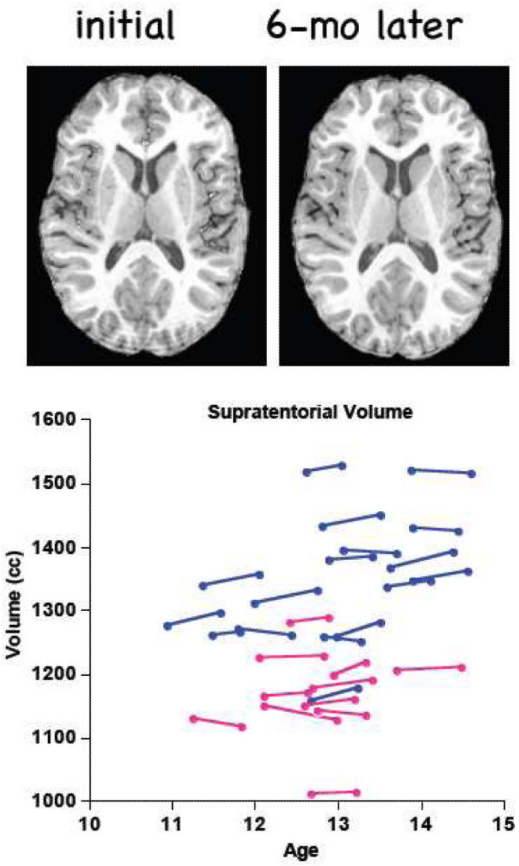

Figure 5.
Top panel: Example of one adolescent's MRIs at the initial and follow-up examination. Bottom panel: “Spaghetti” plot of each subject's supratentorial volumes at each MRI by interval. Blue = boys; pink = girls.

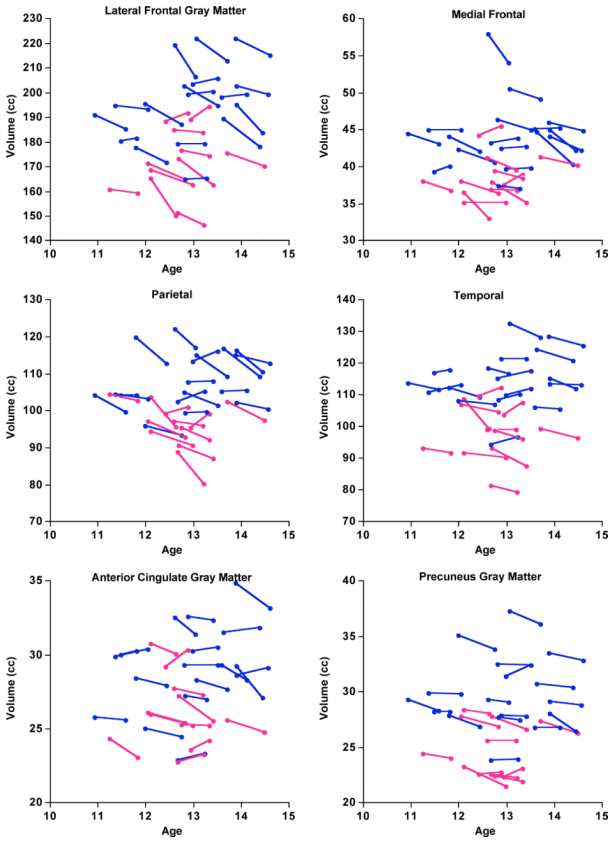

Figure 6.
"Spaghetti" plots of each subject's tissue volumes for ROIs showing significant change between MRIs. Blue = boys; pink = girls.

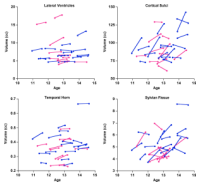

Figure 7.
"Spaghetti" plots of each subject's CSF-filled volumes for ROIs showing significant change between MRIs. Blue = boys; pink = girls.

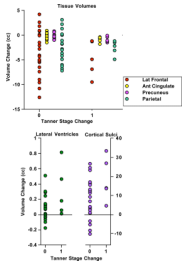

Figure 8.
Four tissue ROIs showing decreases (top panel) and two CSF ROIs showing increases (bottom panel) in the 6 adolescents whose Tanner stage advanced from MRI 1 to MRI 2.

Table 1

Demographic information for each subject group

		Age (years)	Height (cm)	Weight (kg)	BMI (kg/m2)[a]	Tanner Stage	Grade (year)	SES[b]	PPVT IQ[c]	Follow-up Interval (months)
Total N=28	**mean**	11.9	160.0	49.6	19.2	2.8	7.0	21.4	120.9	7.3
	sd	0.8	8.2	9.6	2.5	0.9	0.8	8.5	10.1	1.6
	min	10	143	32.0	15.6	1	5	11	104	4.1
	max	13	174	66.3	25.0	4	8	46	138	10.7
Girls N=12	**mean**	11.8	158.6	47.2	18.7	3.4	6.8	21.5	119.1	6.8
	sd	0.6	6.9	7	1.9	0.5	0.6	4.4	8.0	1.1
	min	11	149	38	16.3	3	6	15	108	5.3
	max	13	170	63	22.4	4	8	29	132	9.4
Boys N=16	**mean**	12.0	161.1	51.3	19.6	2.3	7.1	21.2	122.2	7.0
	sd	0.9	9.2	11.1	2.9	0.8	0.9	10.8	11.5	1.2
	min	10	143	32	15.6	1	5	11	104	4.7
	max	13	174	66.3	25.0	4	8	46	138	9.0
	value	0.42	0.44	0.27	0.38	0.0003	0.33	0.93	0.43	0.18

[a] BMI obesity cut-off varies by sex and age; 1, 11 year old boy and 1, 12 year old boy were at the cusp of the overweight/obesity range (http://www.cdc.gov/obesity/childhood/index.html)

[b] Lower values = higher socioeconimic status (SES)

[c] PPVT IQ = Peabody Picture Vocabulary Test Standard Score IQ equivalent

Table 2

Percent volume change by sequential registration method for each ROI

	Mean % Change	S.D.	t-value	p-value
Lateral Frontal Cortex	−2.38	2.81	−4.4762	0.0001
Medial Frontal Cortex	−2.54	3.45	−3.8940	0.0006
Insula	−0.41	2.91	−0.7453	0.4625
Anterior Cingulate Cortex	−1.27	2.79	−2.3995	0.0236
Posterior Cingulate Cortex	−0.62	4.07	−0.8118	0.4240
Precuneus	−1.56	2.37	−3.4749	0.0017
Hippocampus+Amygdala	0.57	1.51	1.9928	0.0565
Occipital Cortex	0.40	4.06	0.5236	0.6049
Parietal Cortex	−2.57	3.25	−4.1800	0.0003
Caudate+Putamen	0.85	1.01	4.4857	0.0001
Thalamus	1.50	1.69	4.6919	0.0001
Temporal Cortex	−1.08	2.67	−2.1450	0.0411
Superior Cerebellum	0.45	12.80	1.8638	0.0733
Inferior Cerebellum	1.45	2.30	3.2664	0.0031
Calcarine Cortex	2.00	4.40	2.4027	0.0234
Lateral Ventricles	1.66	2.54	3.4583	0.0018
Temporal Horn	2.49	3.62	3.6446	0.0011
Third Ventricle	1.61	7.17	1.1871	0.2455
Cortical Sulci	11.12	12.94	4.5484	0.0001
Sylvian Fissure	7.07	11.96	3.1286	0.0042
Supratentorial Volume	0.95	1.03	4.8736	0.0001